Optical excitation cross section of erbium in GaN

I-Wen Feng,[1] Jing Li,[1] Jingyu Lin,[1] Hongxing Jiang,[1,*] and John Zavada[2]

[1]Department of Electrical and Computer Engineering, Texas Tech University, Lubbock, Texas 79409, USA

[2]Department of Electrical and Computer Engineering, Polytechnic Institute of New York University, Brooklyn, New York 11201, USA

*Corresponding author: hx.jiang@ttu.edu

Received 15 November 2012; revised 11 January 2013; accepted 14 January 2013; posted 14 January 2013 (Doc. ID 179777); published 11 February 2013

Epilayers of erbium-doped GaN (GaN:Er) were synthesized by metal-organic chemical vapor deposition, and the optical excitation cross section (σ_{exc}) of Er ions in this host material were determined. Photoluminescence (PL) measurements were made using laser diodes at excitation wavelengths of 375 and 405 nm, and the integrated emission intensity at 1.54 μm was measured as a function of excitation photon flux. Together with time-resolved PL measurements, values of σ_{exc} of Er ions in GaN:Er were obtained. For excitation at 375 nm, the observed excitation cross section was found to be 4.6×10^{-17} cm^{-2}, which is approximately three orders of magnitude larger than that using resonant excitation. Based on the present and previous works, the optical excitation cross section σ_{exc} of Er ions in GaN:Er as a function the excitation wavelength has been obtained. The large values of σ_{exc} with near-band-edge excitation makes GaN:Er attractive for realization of chip-scale photonic devices for optical communications. © 2013 Optical Society of America

OCIS codes: 160.5690, 160.4760.

1. Introduction

Rare earth (RE)—doped semiconductors have received considerable attention due to the intra-4*f* transitions of these trivalent ions that occur in the visible and infrared spectral regions (see [1] and references therein). The outer 5*s* and 5*p* electronic shells shield the 4*f* electrons, and narrow spectral line emissions are allowed in the presence of the crystal field induced by the host materials [2]. The 1.54 μm emission of erbium ions (Er^{3+}), originating through the intra-4*f* transitions from the first excited manifold ($^4I_{13/2}$) to the ground state ($^4I_{15/2}$), coincides with the minimal-optical-loss band of silica fibers. Different nonsemiconductor materials have been doped with RE atoms for various optoelectronic devices, including silica for erbium-doped fiber amplifiers (EDFAs) [3]. In general, resonant excitation, at 980 or 1480 nm, provides to a small optical excitation cross section of 10^{-20} to 10^{-21} cm^{-2} in optical fibers, and a long waveguide length is needed for the construction of such optical devices [4,5].

Er-doped semiconductors have been widely studied as alternative materials for optical communications. Among various semiconductor host materials, the III-nitride semiconductors exhibit superior room-temperature performance because their large energy bandgaps lead to a lower thermal quenching of Er emission [6–8]. Previously, we reported the synthesis of Er-doped GaN (GaN:Er) by metal–organic chemical vapor deposition (MOCVD) and the strong 1.54 μm emission using above-bandgap excitation [9,10]. The optical cross sections are fundamental parameters that determine the optical properties of devices made of GaN:Er materials. In this work, the optical excitation cross section σ_{exc} and the effective decay lifetime τ of the Er emission at 1.54 μm in GaN:Er epilayers have been investigated. Photoluminescence (PL) measurements of the integrated emission intensity at 1.54 μm were made as a function of excitation photon flux. Coupled with time-resolved PL measurements, values of the σ_{exc} of Er ions under near-bandgap excitation were obtained.

1559-128X/13/061132-04$15.00/0
© 2013 Optical Society of America

2. Experimental Details

GaN:Er epilayers with a thickness of 500 nm were grown on AlN/Al_2O_3 templates by MOCVD at 1020°C. Trimethylgallium (TMGa), tris-isopropylcyclopentadienylerbium (TRIPEr), and ammonia (NH_3) were used as the group-III, Er dopant and group-V precursors, respectively, and were carried into the MOCVD reactor by H_2 gas. For the infrared PL measurements, two laser diodes having excitation wavelengths (λ_{exc}) of $\lambda_{exc} = 375$ nm (LDCU 8646) and $\lambda_{exc} = 405$ nm (Thorlabs CPS-405) were used as excitation sources. A thermoelectric-cooled infrared spectrometer (Bayspec deep-cooled InGaAs NIR spectrometer) was used to disperse the PL emission spectra. To probe the rise and decay kinetics of the 1.54 μm emission line, time-resolved PL measurements were conducted, and a square electrical pulse with 20 ms width and 10 Hz frequency was used to drive the diode lasers. A low-power germanium photodetector, used to measure the time-dependent 1.54 μm emission, was connected to a low-noise current preamplifier and a digital oscilloscope to convert the optical emission intensity into an electrical signal. The overall system response time is around 50 μs.

3. Results and Discussions

Figure 1 shows typical PL spectra near 1.54 μm of GaN:Er epilayers at an excitation power of ~1.6 mW. It is apparent that the 1.54 μm emission is stronger for $\lambda_{exc} = 375$ nm than for $\lambda_{exc} = 405$ nm by a factor of about four, which is consistent with our previous results using light-emitting diodes with various λ_{exc} as excitation sources [11]. Figure 2(a) shows the 1.54 μm emission spectra, and Fig. 2(b) shows the integrated 1.54 μm emission intensity I_{int} measured from a GaN:Er epilayer as a function of excitation photon flux φ_{exc} with $\lambda_{exc} = 375$ nm. As expected, I_{int} increases with an increase of φ_{exc}. The optical excitation process of Er^{3+} atoms can be expressed by

$$\frac{dN^*_{Er}}{dt} = \sigma_{exc}\varphi_{exc}(N_{Er} - N^*_{Er}) - \frac{N^*_{Er}}{\tau}, \quad (1)$$

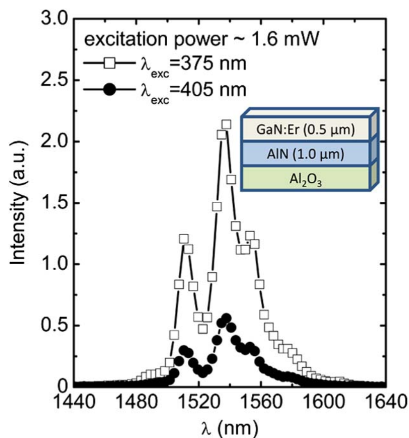

Fig. 1. (Color online) Infrared PL spectra near 1.54 μm measured from a GaN:Er epilayer at an excitation power ~1.6 mW for $\lambda_{exc} =$ 375 and 405 nm. The schematic structure diagram of the GaN:Er epilayer grown on an AlN/sapphire template is shown in the inset.

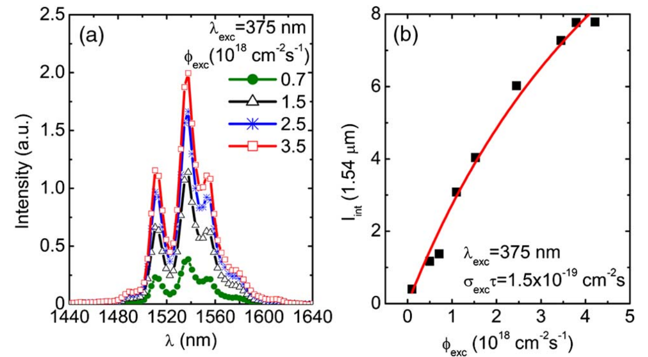

Fig. 2. (Color online) (a) Infrared PL emission spectra near 1.54 μm and (b) integrated 1.54 μm emission intensity I_{int} measured from a GaN:Er epilayer as a function of the excitation photon flux φ_{exc} for $\lambda_{exc} = 375$ nm. The solid curve is the least squares fit of data using Eq. (2).

where N^*_{Er} is the excited Er^{3+} concentration and N_{Er} is the total concentration of the optically active Er^{3+} centers [12–15]. As the steady state is reached, I_{int} can be expressed as

$$I_{int} \propto \frac{N^*_{Er}}{\tau_{rad}} = \left(\frac{\sigma_{exc}\tau\varphi_{exc}}{\sigma_{exc}\tau\varphi_{exc} + 1}\right)\frac{N_{Er}}{\tau_{rad}}, \quad (2)$$

where τ_{rad} refers to the radiative decay lifetime and can be described as $1/\tau = 1/\tau_{rad} + 1/\tau_{nonrad}$ (where τ_{nonrad} refers to the nonradiative decay lifetime). Equation (2) describes the measured data very well. The solid curve in Fig. 2(b) is the least squares fit of the measured I_{int} as a function of φ_{exc} using Eq. (2). The best fit was found with $\sigma_{exc}\tau = 1.5 \times 10^{-19}$ cm^{-2} s for $\lambda_{exc} = 375$ nm.

The rise and decay kinetics of the 1.54 μm emission line were probed using time-resolved PL measurements to provide the values of σ_{exc} and τ separately for $\lambda_{exc} = 375$ nm. Figure 3(a) shows time-resolved PL measurement data for $\lambda_{exc} = 375$ nm for different φ_{exc}. When the excitation is on ($t = 0 - 20$ ms), the 1.54 μm emission intensity increases with time

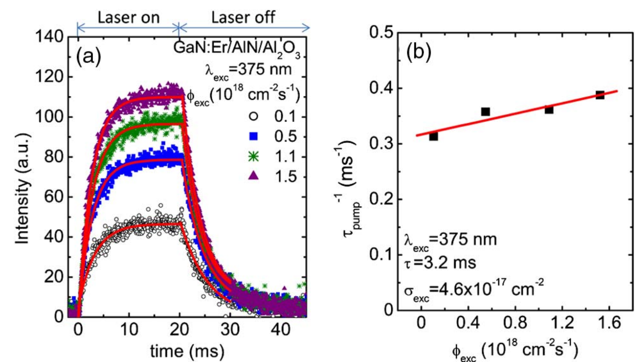

Fig. 3. (Color online) (a) Rise and decay kinetics of the 1.54 μm emission line probed using time-resolved PL measurements and (b) reciprocal value of the characteristic rising time τ^{-1}_{pump} as a function of the excitation photon flux φ_{exc} for $\lambda_{exc} = 375$ nm measured from a GaN:Er epilayer sample. The solid curves are the least squares fit of data using Eqs. (3)–(5).

and approaches a saturation level for $t > 10$ ms. A further increase in φ_{exc} only leads to a slightly higher saturation level. The measured I_{int} as a function of time in the turn-on (excitation) time period can be described as

$$I(t) = I_0\left(1 - \exp\left(-\frac{t}{\tau_{pump}}\right)\right), \tag{3}$$

where τ_{pump} and I_0 refer, respectively, to the characteristic rising time and to the saturation emission intensity ($t \to \infty$) under different φ_{exc}. The solid curves in Fig. 3(a) are the least squares fit of the measured time-dependent intensity data using Eq. (3), from which τ_{pump} under various φ_{exc} can thus be obtained. The reciprocal τ_{pump} value is plotted as a function of φ_{exc} for $\lambda_{exc} = 375$ nm in Fig. 3(b). It was observed that τ_{pump}^{-1} values increase with an increase of φ_{exc}, which implies faster saturation processes for the 1.54 μm emission under higher φ_{exc}. By solving Eq. (1), τ_{pump}^{-1} can be expressed as

$$\tau_{pump}^{-1} = \sigma_{exc}\varphi_{exc} + \frac{1}{\tau}. \tag{4}$$

The solid line in Fig. 3(b) is a least squares fit of data using Eq. (4). The best fit values of τ and σ_{exc} for $\lambda_{exc} = 375$ nm are $\tau = 3.2$ ms and $\sigma_{exc} = 4.6 \times 10^{-17}$ cm^{-2}, respectively. The value of $\sigma_{exc}\tau$ obtained from the PL rising kinetics is thus $\sigma_{exc}\tau = 1.47 \times 10^{-19}$ cm^{-2} s, which is in excellent agreement with that obtained from the relation between the measured I_{int} and φ_{exc} shown in Fig. 2(b) using Eq. (2) ($\sigma_{exc}\tau = 1.5 \times 10^{-19}$ cm^{-2} s). This provides high confidence of our analysis. On the other hand, the PL decay kinetics (during the turn-off period) of 1.54 μm emission can be described by an exponential decrease with time,

$$I(t) = I_0 \exp(-t/\tau), \tag{5}$$

as illustrated in Fig. 3(a).

For comparison, τ and σ_{exc} of Er in the same GaN:Er epilayers for $\lambda_{exc} = 405$ nm were also estimated through PL and time-resolved PL measurements as shown in Fig. 4(a). Figure 4(b) plots the measured I_{int} of the 1.54 μm emission as a function of φ_{exc} for $\lambda_{exc} = 405$ nm. As expected, an increase of φ_{exc} leads to a stronger 1.54 μm emission. The line with open squares in Fig. 4(b) is the least squares fit of data using Eq. (2). The best fit value of $\sigma_{exc}\tau$ with $\lambda_{exc} = 405$ nm is $\sigma_{exc}\tau = 7.1 \times 10^{-20}$ cm^{-2} s. To obtain the values of σ_{exc} and τ separately with $\lambda_{exc} = 405$ nm pumping, we plot the measured τ_{pump}^{-1} from time-resolved PL as a function of φ_{exc} for $\lambda_{exc} = 405$ nm in Fig. 4(b). Similarly, an increase of φ_{exc} also leads to a shorter rising time to reach the saturation level, as described by Eq. (4). The line with solid circles in Fig. 4(b) is the least squares fit of data with Eq. (4). The fitted values of τ and σ_{exc} are $\tau = 3.8$ ms and

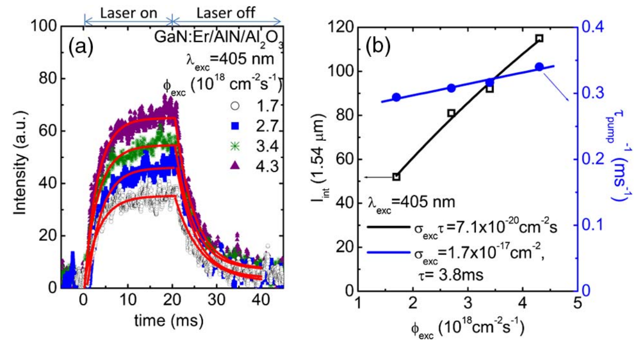

Fig. 4. (Color online) Rise and decay kinetics of the 1.54 μm emission line probed using time-resolved PL measurements and (b) integrated 1.54 μm emission intensity I_{int} and the reciprocal value of the characteristic rising time τ_{pump}^{-1} as a function of the excitation photon flux φ_{exc} for $\lambda_{exc} = 405$ nm measured from a GaN:Er epilayer sample. The solid lines are the least squares fit of data using Eqs. (2)–(5).

$\sigma_{exc} = 1.7 \times 10^{-17}$ cm^{-2}. Consequently, the value of $\sigma_{exc}\tau$ is $\sigma_{exc}\tau = 7.1 \times 10^{-20}$ cm^{-2} s for $\lambda_{exc} = 405$ nm. This smaller value of σ_{exc} for $\lambda_{exc} = 405$ nm compared with that for $\lambda_{exc} = 375$ nm explains the results of lower optical pumping efficiency of the 1.54 μm emission for $\lambda_{exc} = 405$ nm shown in Fig. 1.

With the above- or near-bandgap excitation, the dominant excitation mechanism of the 1.54 μm emission in GaN:Er is due to the exchange of energy between the electrons captured by the complexes involving Er and nitrogen vacancies (Er_{Ga}–V_N) and the 4*f* core states of Er [10,15]. Thus, the presence of a higher photoexcited electron density translates to a higher optical cross section. Because the relative optical absorption coefficient and hence the photoexcited carrier density decrease exponentially with excitation photon energy near the band edge [11,15], the excitation cross section φ_{exc} at $\lambda_{exc} = 375$ nm is expected to be higher than that at $\lambda_{exc} = 405$ nm, which is what we observed. Based on Eq. (4), a larger excitation cross section naturally leads to a shorter effective decay lifetime at $\lambda_{exc} = 375$ nm than at $\lambda_{exc} = 405$ nm.

Based on the present and previous studies [15,16], we have obtained the optical excitation cross section σ_{exc} of Er ions in GaN host as a function of the excitation wavelength λ_{exc}, and the results are summarized in Fig. 5. Under a resonant excitation ($\lambda_{exc} = 980$ or 1480 nm), the 1.54 μm emission is limited by the small absorption cross section of Er^{3+} atoms [16]. On the other hand, with the above or near-bandgap excitation, Er^{3+} atoms are excited through carriers generated by optical absorption in the GaN host. In this case, σ_{exc} is determined by the absorption coefficient of GaN, which is very large and decreases exponentially with a decrease of the excitation photon energy [15]. This result of exponential decrease of σ_{exc} with an increase of λ_{exc} explains very well our earlier results, which showed an approximately exponential decrease of the 1.54 μm emission intensity with a decrease of the excitation photon energy in the band-edge region [11].

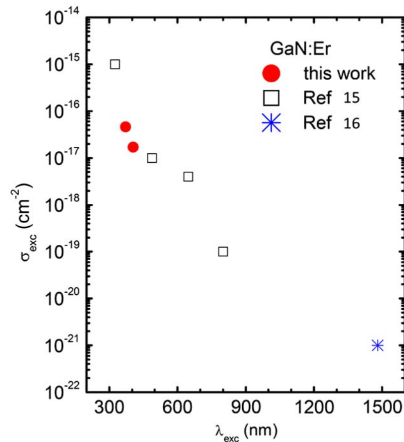

Fig. 5. (Color online) Excitation wavelength (λ_{exc})-dependent optical excitation cross section σ_{exc} of GaN:Er epilayers, including the results in this work and previous results [15,16].

4. Summary and Conclusions

In summary, the optical excitation cross section σ_{exc} of Er in GaN epilayers grown by MOCVD has been studied. The determined value of $\sigma_{exc} = 4.6 \times 10^{-17}$ cm^{-2} s for $\lambda_{exc} = 375$ nm is approximately three orders of magnitude larger than that using a resonant excitation ($\lambda_{exc} = 980$ nm or 1480 nm). While EDFAs are an established technology, they are difficult to integrate with many other functional photonic devices because a long waveguide length is needed for resonant excitation due to the small excitation cross section and limited Er doping concentration. In contrast, Er-doped III-nitride semiconductors with above- or near-band-edge excitation via laser diode pump or current injection could be an attractive alternative approach to achieve chip-scale infrared emitters and optical amplifiers for optical communications [17]. If realized, GaN:Er-based devices would lead to integration with other functional optical devices, such as wavelength routers, optical switches, light sources, and detectors, to build monolithic photonic integrated circuits.

The materials growth effort is supported by JTO/ARO (W911NF-12-1-0330), and the optical characterization work is supported by NSF (ECCS-1200168). HXJ and JYL thank the AT&T Foundation for the support of the Ed Whitacre and Linda Whitacre endowed chairs. JMZ acknowledges support from NSF under the IR/D program. Any conclusions in this paper do not necessarily reflect the views of NSF/JTO/ARO.

References

1. P. Ruterana, ed., *Rare Earth Doped Materials for Photonics: Proceedings of E-MRS Symposium Spring 2003* (Elsevier 2003).
2. G. H. Dicke, *Spectra and Energy Levels of Rare Earth Ion in Crystals* (Interscience, 1968).
3. E. Desurvire, *Erbium-Doped Fibre Amplifiers: Principles and Applications* (Wiley, 1994).
4. E. Snoeks, G. N. van den Hoven, A. Polman, B. Hendriksen, M. B. J. Diemeer, and F. Priolo, "Cooperative upconversion in erbium-implanted soda-lime silicate glass optical waveguides," J. Opt. Soc. Am. B **12**, 1468–1474 (1995).
5. A. R. Peaker, "Erbium in semiconductors: where are we coming from; where are we going," Mater. Res. Soc. Symp. Proc. **866**, 3–12 (2005).
6. P. Favennec, H. Lharidon, D. Moutonnet, M. Salvi, and M. Gauneau, "Optical activation of Er^{3+} implanted in silicon by oxygen impurities," Jpn. J. Appl. Phys. **29**, L524–L526 (1990).
7. M. Thaik, U. Hommerich, R. N. Schwartz, R. G. Wilson, and J. M. Zavada, "Photoluminescence spectroscopy of erbium implanted gallium nitride," Appl. Phys. Lett. **71**, 2641–2643 (1997).
8. S. J. Pearton, C. R. Abernathy, J. D. MacKenzie, U. Hömmerich, J. M. Zavada, R. G. Wilson, and R. N. Schwartz, "Effect of atomic hydrogen on Er luminescence from AlN," J. Vac. Sci. Technol. A **16**, 1627–1630 (1998).
9. C. Ugolini, N. Nepal, J. Y. Lin, H. X. Jiang, and J. M. Zavada, "Erbium-doped GaN epilayers synthesized by metal-organic chemical vapor deposition," Appl. Phys. Lett. **89**, 151903 (2006).
10. C. Ugolini, N. Nepal, J. Y. Lin, H. X. Jiang, and J. M. Zavada, "Excitation dynamics of the 1.54 μm emission in Er doped GaN synthesized by metal organic chemical vapor deposition," Appl. Phys. Lett. **90**, 051110 (2007).
11. R. Dahal, C. Ugolini, J. Y. Lin, H. X. Jiang, and J. M. Zavada, "Current-injected 1.54 μm light emitting diodes based on erbium-doped GaN," Appl. Phys. Lett. **93**, 033502 (2008).
12. F. Priolo, G. Franzò, S. Coffa, and A. Carnera, "Excitation and nonradiative deexcitation processes of Er^{3+} in crystalline Si," Phys. Rev. B **57**, 4443–4455 (1998).
13. G. Franzo, S. Coffa, F. Priolo, and C. Spinella, "Mechanism and performance of forward and reverse bias electroluminescence at 1.54 μm from Er-doped Si diodes," J. Appl. Phys. **81**, 2784–2793 (1997).
14. O. B. Gusev, M. S. Bresler, P. E. Pak, I. N. Yassievich, M. Forcales, N. Q. Vinh, and T. Gregorkiewicz, "Excitation cross section of erbium in semiconductor matrices under optical pumping," Phys. Rev. B **64**, 075302 (2001).
15. A. Braud, "Excitation mechanisms of re ions in semiconductors," in *Topics in Applied Physics: Rare Earth Doped III-Nitrides for Optoelectronic and Spintronic Applications*, K. O'Donnell and V. Dierolf, eds.(Springer, 2010), pp. 269–308.
16. Q. Wang, R. Dahal, I.-W. Feng, J. Y. Lin, H. X. Jiang, and R. Hui, "Emission and absorption cross-sections of an Er:GaN waveguide prepared with metal organic chemical vapor deposition," Appl. Phys. Lett. **99**, 121106 (2011).
17. R. Dahal, J. Y. Lin, H. X. Jiang, and J. M. Zavada, "Er-doped GaN and InGaN for optical communications," in *Topics in Applied Physics: Rare Earth Doped III-Nitrides for Optoelectronic and Spintronic Applications*, K. O'Donnell and V. Dierolf, eds. (Springer, 2010), pp. 116–157.